Biomedical Optics EXPRESS

Effects of tissue heterogeneity on the optical estimate of breast density

Paola Taroni,[1,*] Antonio Pifferi,[1,2] Giovanna Quarto,[1] Lorenzo Spinelli,[2] Alessandro Torricelli,[1] Francesca Abbate,[3] Nicola Balestreri,[4] Serena Ganino,[3] Simona Menna,[3] Enrico Cassano,[3] and Rinaldo Cubeddu,[1,2]

[1]*Dipartimento di Fisica, Politecnico di Milano, Piazza Leonardo da Vinci 32, 20133 Milano, Italy*
[2]*Istituto di Fotonica e Nanotecnologie, Consiglio Nazionale delle Ricerche, Piazza Leonardo da Vinci 32, 20133 Milano, Italy*
[3]*European Institute of Oncology, Division of Breast Radiology, Via G. Ripamonti, 435, 20141 Milano, Italy*
[4]*European Institute of Oncology, Department of Radiology, Via G. Ripamonti, 435, 20141 Milano, Italy*
**paola.taroni@fisi.polimi.it*

Abstract: Breast density is a recognized strong and independent risk factor for developing breast cancer. At present, breast density is assessed based on the radiological appearance of breast tissue, thus relying on the use of ionizing radiation. We have previously obtained encouraging preliminary results with our portable instrument for time domain optical mammography performed at 7 wavelengths (635–1060 nm). In that case, information was averaged over four images (cranio-caudal and oblique views of both breasts) available for each subject. In the present work, we tested the effectiveness of just one or few point measurements, to investigate if tissue heterogeneity significantly affects the correlation between optically derived parameters and mammographic density. Data show that parameters estimated through a single optical measurement correlate strongly with mammographic density estimated by using BIRADS categories. A central position is optimal for the measurement, but its exact location is not critical.

OCIS codes: (170.6510) Spectroscopy, tissue diagnostics; (170.6935) Tissue characterization; (170.3830) Mammography; (170.5280) Photon migration.

References and links

1. J. Ferlay, D. M. Parkin, and E. Steliarova-Foucher, "Estimates of cancer incidence and mortality in Europe in 2008," Eur. J. Cancer **46**(4), 765–781 (2010).
2. A. Jemal, R. Siegel, J. Xu, and E. Ward, "Cancer statistics, 2010," CA Cancer J. Clin. **60**(5), 277–300 (2010).
3. V. A. McCormack and I. dos Santos Silva, "Breast density and parenchymal patterns as markers of breast cancer risk: a meta-analysis," Cancer Epidemiol. Biomarkers Prev. **15**(6), 1159–1169 (2006).
4. N. F. Boyd, L. J. Martin, J. Stone, C. Greenberg, S. Minkin, and M. J. Yaffe, "Mammographic densities as a marker of human breast cancer risk and their use in chemoprevention," Curr. Oncol. Rep. **3**(4), 314–321 (2001).
5. M. K. Simick, R. Jong, B. Wilson, and L. Lilge, "Non-ionizing near-infrared radiation transillumination spectroscopy for breast tissue density and assessment of breast cancer risk," J. Biomed. Opt. **9**(4), 794–803 (2004).
6. K. M. Blackmore, J. A. Knight, and L. Lilge, "Association between transillumination breast spectroscopy and quantitative mammographic features of the breast," Cancer Epidemiol. Biomarkers Prev. **17**(5), 1043–1050 (2008).
7. S. Alowami, S. Troup, S. Al-Haddad, I. Kirkpatrick, and P. H. Watson, "Mammographic density is related to stroma and stromal proteoglycan expression," Breast Cancer Res. **5**(5), R129–R135 (2003).
8. P. Taroni, A. Pifferi, G. Quarto, L. Spinelli, A. Torricelli, F. Abbate, A. Villa, N. Balestreri, S. Menna, E. Cassano, and R. Cubeddu, "Noninvasive assessment of breast cancer risk using time-resolved diffuse optical spectroscopy," J. Biomed. Opt. **15**(6), 060501 (2010).
9. J. R. Mourant, T. Fuselier, J. Boyer, T. M. Johnson, and I. J. Bigio, "Predictions and measurements of scattering and absorption over broad wavelength ranges in tissue phantoms," Appl. Opt. **36**(4), 949–957 (1997).
10. A. M. Nilsson, C. Sturesson, D. L. Liu, and S. Andersson-Engels, "Changes in spectral shape of tissue optical properties in conjunction with laser-induced thermotherapy," Appl. Opt. **37**(7), 1256–1267 (1998).
11. P. Taroni, A. Pifferi, E. Salvagnini, L. Spinelli, A. Torricelli, and R. Cubeddu, "Seven-wavelength time-resolved optical mammography extending beyond 1000 nm for breast collagen quantification," Opt. Express **17**(18), 15932–15946 (2009).

#174025 - $15.00 USD Received 8 Aug 2012; revised 3 Sep 2012; accepted 3 Sep 2012; published 6 Sep 2012

12. B. Zheng, J. H. Sumkin, M. L. Zuley, X. Wang, A. H. Klym, and D. Gur, "Bilateral mammographic density asymmetry and breast cancer risk: A preliminary assessment," Eur. J. Radiol. (to be published).

1. Introduction

Breast cancer is the most common cancer among women, and the second leading cause of death in several countries [1,2]. Breast density is a recognized independent risk factor for developing breast cancer [3,4]. Including it into risk prediction models improves their prediction accuracy, and improved risk models could be used to better address not only closer screening of high-risk women, but also prevention of breast cancer.

The assessment of breast density presently requires the use of ionizing radiation (x-ray mammography), while optical techniques could provide a noninvasive means for its estimate. In this line, Lilge and colleagues collected continuous wave (CW) transmittance data over a broad spectral range (550–1300 nm) and interpreted them using principal component analysis. This provided a very good correlation with quantitative mammographic features [5,6].

We are also performing a clinical study for the optical assessment of breast density, with a 7-wavelength (635–1060 nm) time domain instrument. Based on preliminary results, excellent agreement can be achieved between mammographic density and an optical index based on tissue composition and scattering parameters, as derived from optical measurements. Moreover, changes in density are expected to reflect stromal changes [7] and collagen is related to stromal changes. Direct correlation was observed between mammographic density and optically quantified collagen content, which thus deserves further investigation as a potential means for the direct assessment of cancer risk [8].

For the estimate of breast density both CW and time domain data were averaged over multiple measurement positions. CW transmittance information were acquired in 4 selected positions per breast (representing medial, distal, lateral and central quadrants) and averaged after data processing with principle component analysis [5,6]. Time domain transmittance data were collected scanning the entire breast both in cranio-caudal and oblique (45°) views. Tissue composition and scattering parameters were estimated at each pixel position (*i.e.*, every millimeter) and finally averaged [8]. Thus, in both cases average over the heterogeneous properties of breast tissue was performed, in line with the assessment of mammographic density either through BIRADS categories or percentage evaluation.

Aim of the present study is to investigate breast tissue heterogeneity and determine if a single point transmittance measurement can still provide an overall characterization of breast tissue, and consequently allow a reliable estimate of breast density, in good agreement with the mammographic assessment, at least in the case of time domain acquisition and following data processing.

2. Data acquisition and analysis

Our portable clinical instrument for time domain optical mammography operates in transmittance geometry on the mildly compressed breast. Time-resolved transmittance data are collected at 7 wavelengths in the range 635–1060 nm, using picosecond pulsed diode lasers as light sources, and two photomultiplier tubes and PC boards for time-correlated single photon counting to detect the time distributions of the transmitted pulses. Injection and collection fibers are scanned in tandem over the compressed breast and data are stored every millimeter. Images are routinely acquired from both breasts in cranio-caudal (CC) and oblique (OB, 45°) views.

Data analysis includes the interpretation of time-resolved spectral data with a spectrally constrained global fitting procedure that relies on the diffusion theory for a homogeneous medium to estimate tissue composition in terms of oxy- and deoxyhemoglobin (HbO_2 and Hb, respectively), water, lipids and collagen content, as well as scattering parameters (scattering amplitude a and power b, where the reduced scattering coefficient is described as $\mu_s' = a\lambda^{-b}$) [9,10]. Moreover, for the detection of breast lesions, scattering maps are routinely applied, together with late gated intensity images that are sensitive to spatial changes in the absorption properties. The estimate of the optical properties and of tissue composition and structure is

#174025 - $15.00 USD Received 8 Aug 2012; revised 3 Sep 2012; accepted 3 Sep 2012; published 6 Sep 2012

limited to a reference area that excludes boundaries and marked inhomogeneities, but still includes most of the scanned breast volume. The time-of-flight (*i.e.* the first moment of the time-resolved transmittance curve) is calculated for each image pixel, and only pixels with time-of-flight greater than or equal to the median of the distribution are included in the reference area.

Details on the instrument set-up and performances, and on the procedures for data acquisition and analysis are reported in Ref. [11].

The optical mammograph is presently applied in a clinical study approved by the Institutional Review Board of the European Institute of Oncology. Written informed consent is obtained from all patients. The study has two-fold aim: the optical characterization of malignant and benign breast lesions and the noninvasive assessment of breast density. Thus both healthy subjects and patients with breast lesions are included in the study. Routine data analysis for the estimate of breast density involves the average of optically derived parameters over all four images (cranio-caudal and oblique views of both breasts) available for each subject, so as to provide the average optical properties and breast tissue composition of that subject.

To investigate the effects of breast heterogeneity on the assessment of breast density, data collected from the first 60 subjects of the study were considered. General patient information is reported in Table 1.

For the present study, correlation with mammographic density was estimated not only from full scan optical data, but also from optical parameters averaged only over small (5 mm × 5 mm) areas, selected on the CC views of both breasts. Five different locations were identified, as shown in Fig. 1, and are labeled 1, Outer; 2, Chest; 3, Inner; 4, Nipple; 5, Middle. In the case of 4 subjects, due to the small breast volume, partial overlap of some areas occurred. Thus they were excluded from further analysis.

Table 1. General statistics of the patient population

Item	Value
Subjects (#)	60
Age (y)	52.6 ± 12.2
BMI (kg/m^2)	23.4 ± 3.7
Premenopausal status (#)	25

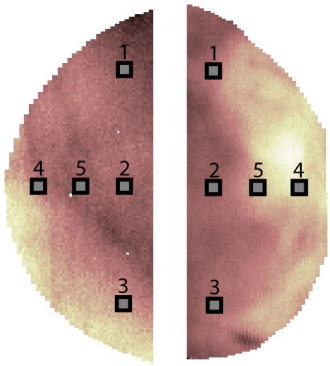

Fig. 1. Selection of the 5 areas that simulate point measurements on the cranio-caudal views of the right and left breasts of a subject.

Recent x-ray mammograms were not available for 4 more patients. Thus they were also excluded from further analysis. Therefore full analysis was performed on data collected from 52 subjects. An expert radiologist assigned Breast Imaging and Reporting Data System (BIRADS) mammographic density categories as: (i) almost entirely fat (category 1, $n = 8$); (ii) scattered fibroglandular densities (category 2, $n = 19$); (iii) heterogeneously dense (category 3, $n = 16$); and (iv) extremely dense (category 4, $n = 9$).

#174025 - $15.00 USD Received 8 Aug 2012; revised 3 Sep 2012; accepted 3 Sep 2012; published 6 Sep 2012

3. Results and discussion

To determine if tissue heterogeneity affects the estimate of breast density we considered all optically derived parameters, concerning both tissue composition (in terms of water, lipid, collagen, and total hemoglobin content *tHb* and oxygenation SO_2) and scattering properties (scattering amplitude *a* and power *b*).

Full scan data acquired every millimeter in CC and OB views from both breasts were available for all subjects. We choose to average data included in 5 mm × 5 mm areas selected on the CC views to mimic single point measurements performed with a fiber bundle.

As a first step, we evaluated the average values of all parameters as a function of mammographic density (BIRADS categories 1 to 4) and measurement position (Areas 1 to 5, as defined previously, for both the left and right CC views). As expected, tissue composition and scattering parameters change progressively upon increasing BIRADS category. In particular, in agreement with what already observed previously for full scan data [8], water and collagen content as well as the scattering power increase with mammographic density, while lipid content progressively decrease (Tables 2–5).

Average values corresponding to each BIRADS category also depend on the measurement position and, at least in part, the observed changes reflect breast anatomy. As an example, content of both water and collagen is higher in the outer quadrant (area 1) than in the inner one (area 3) (Tables 2 and 3). Opposite behavior is observed for lipid (Table 4). These differences in tissue composition are consistent with the expected higher percentage of fibroglandular tissue in the outer quadrant.

Table 2. Water content (mg/cm^3) as a function of measurement position and BIRADS category

CC View	BIRADS category	1 Outer	2 Chest	3 Inner	4 Nipple	5 Middle	All areas	Full scan
Left	1	74 ± 21	80 ± 22	74 ± 15	87 ± 31	84 ± 22	80 ± 21	80 ± 22
	2	107 ± 61	107 ± 55	94 ± 43	114 ± 76	108 ± 58	106 ± 59	107 ± 55
	3	233 ± 136	208 ± 114	153 ± 67	238 ± 146	216 ± 114	210 ± 120	210 ± 106
	4	456 ± 157	445 ± 162	303 ± 122	539 ± 180	509 ± 145	449 ± 169	435 ± 131
	All	201 ± 168	192 ± 159	146 ± 103	224 ± 197	199 ± 169	192 ± 163	193 ± 150
Right	1	73 ± 19	78 ± 19	69 ± 21	82 ± 29	78 ± 21	76 ± 21	77 ± 22
	2	112 ± 57	111 ± 54	94 ± 39	128 ± 92	120 ± 61	113 ± 63	112 ± 58
	3	216 ± 144	207 ± 102	155 ± 74	263 ± 142	228 ± 111	214 ± 120	212 ± 104
	4	460 ± 124	474 ± 135	328 ± 123	527 ± 127	493 ± 121	456 ± 139	452 ± 109
	All	198 ± 165	198 ± 160	149 ± 111	232 ± 186	209 ± 165	197 ± 160	198 ± 152

Table 3. Collagen content (mg/cm^3) as a function of measurement position and BIRADS category

CC View	BIRADS category	1 Outer	2 Chest	3 Inner	4 Nipple	5 Middle	All areas	Full scan
Left	1	49 ± 13	38 ± 14	42 ± 18	52 ± 23	35 ± 18	43 ± 18	44 ± 18
	2	63 ± 24	44 ± 21	51 ± 18	61 ± 31	45 ± 22	53 ± 24	54 ± 22
	3	95 ± 37	77 ± 39	85 ± 33	87 ± 39	75 ± 38	84 ± 37	84 ± 32
	4	137 ± 53	112 ± 47	117 ± 46	128 ± 56	121 ± 52	123 ± 49	121 ± 44
	All	83 ± 45	65 ± 41	72 ± 39	79 ± 45	64 ± 43	73 ± 43	74 ± 40
Right	1	48 ± 19	37 ± 20	47 ± 21	51 ± 25	35 ± 20	43 ± 21	43 ± 22
	2	65 ± 41	46 ± 31	55 ± 27	67 ± 45	49 ± 40	57 ± 38	55 ± 34
	3	88 ± 47	70 ± 37	81 ± 37	85 ± 32	71 ± 36	79 ± 38	82 ± 35
	4	123 ± 38	98 ± 37	110 ± 35	114 ± 39	101 ± 37	109 ± 37	111 ± 36
	All	80 ± 46	61 ± 38	71 ± 38	78 ± 42	62 ± 41	70 ± 41	71 ± 39

#174025 - $15.00 USD Received 8 Aug 2012; revised 3 Sep 2012; accepted 3 Sep 2012; published 6 Sep 2012

Table 4. Lipid content (mg/cm^3) as a function of measurement position and BIRADS category

CC View	BIRADS category	1 Outer	2 Chest	3 Inner	4 Nipple	5 Middle	All areas	Full scan
Left	1	782 ± 22	775 ± 25	765 ± 41	759 ± 32	775 ± 28	772 ± 30	777 ± 20
	2	728 ± 75	735 ± 94	755 ± 73	666 ± 142	724 ± 103	721 ± 103	735 ± 73
	3	599 ± 103	615 ± 93	642 ± 66	549 ± 143	585 ± 125	598 ± 111	626 ± 83
	4	445 ± 100	439 ± 80	548 ± 84	407 ± 113	423 ± 108	453 ± 106	467 ± 93
	All	649 ± 142	654 ± 142	684 ± 106	598 ± 168	644 ± 156	646 ± 146	660 ± 129
Right	1	764 ± 46	773 ± 29	771 ± 36	746 ± 36	778 ± 37	767 ± 37	766 ± 34
	2	715 ± 75	735 ± 79	737 ± 67	674 ± 110	723 ± 80	717 ± 85	725 ± 77
	3	574 ± 174	592 ± 132	653 ± 69	576 ± 90	587 ± 98	596 ± 119	619 ± 74
	4	447 ± 93	440 ± 97	518 ± 82	404 ± 85	432 ± 93	448 ± 94	448 ± 83
	All	633 ± 158	646 ± 151	679 ± 108	608 ± 142	642 ± 144	641 ± 142	649 ± 129

Table 5. Scattering power *b* as a function of measurement position and BIRADS category

CC View	BIRADS category	1 Outer	2 Chest	3 Inner	4 Nipple	5 Middle	All areas	Full scan
Left	1	0.39 ± 0.08	0.33 ± 0.07	0.38 ± 0.10	0.39 ± 0.12	0.38 ± 0.09	0.38 ± 0.09	0.39 ± 0.10
	2	0.45 ± 0.10	0.39 ± 0.09	0.46 ± 0.09	0.48 ± 0.14	0.45 ± 0.09	0.45 ± 0.11	0.46 ± 0.09
	3	0.65 ± 0.14	0.47 ± 0.18	0.75 ± 0.17	0.71 ± 0.23	0.65 ± 0.18	0.70 ± 0.20	0.68 ± 0.23
	4	0.91 ± 0.21	0.71 ± 0.18	0.99 ± 0.10	0.96 ± 0.21	0.89 ± 0.21	0.96 ± 0.20	0.90 ± 0.21
	All	0.58 ± 0.22	0.46 ± 0.23	0.63 ± 0.17	0.61 ± 0.28	0.58 ± 0.24	0.61 ± 0.24	0.59 ± 0.26
Right	1	0.42 ± 0.05	0.38 ± 0.07	0.40 ± 0.05	0.44 ± 0.08	0.41 ± 0.06	0.41 ± 0.06	0.43 ± 0.07
	2	0.51 ± 0.12	0.41 ± 0.10	0.50 ± 0.08	0.53 ± 0.12	0.50 ± 0.11	0.50 ± 0.11	0.54 ± 0.09
	3	0.70 ± 0.37	0.50 ± 0.23	0.79 ± 0.21	0.75 ± 0.21	0.70 ± 0.23	0.68 ± 0.27	0.79 ± 0.20
	4	1.07 ± 0.12	0.87 ± 0.20	1.13 ± 0.24	1.10 ± 0.18	1.04 ± 0.17	1.03 ± 0.20	1.01 ± 0.15
	All	0.65 ± 0.29	0.51 ± 0.27	0.68 ± 0.23	0.68 ± 0.30	0.64 ± 0.27	0.64 ± 0.28	0.68 ± 0.25

Table 6. Total hemoglobin content *tHb* as a function of measurement position and BIRADS category

CC View	BIRADS category	1 Outer	2 Chest	3 Inner	4 Nipple	5 Middle	All areas	Full scan
Left	1	8.4 ± 1.8	8.2 ± 2.5	9.8 ± 2.6	8.3 ± 2.0	7.9 ± 2.0	8.5 ± 2.2	8.5 ± 2.1
	2	10.7 ± 3.3	10.5 ± 3.7	11.7 ± 3.3	10.7 ± 4.1	10.0 ± 3.9	10.7 ± 3.6	10.6 ± 3.4
	3	12.0 ± 2.9	11.8 ± 3.4	14.0 ± 4.3	11.3 ± 3.7	11.6 ± 3.8	12.1 ± 3.7	12.0 ± 3.3
	4	13.3 ± 4.3	12.2 ± 4.1	15.5 ± 4.2	11.7 ± 4.5	11.3 ± 4.5	12.8 ± 4.4	13.0 ± 3.8
	All	11.1 ± 3.5	10.8 ± 3.7	12.8 ± 4.1	10.7 ± 3.9	10.4 ± 3.9	11.1 ± 3.9	11.2 ± 3.5
Right	1	8.3 ± 2.4	7.8 ± 2.0	9.3 ± 2.3	9.0 ± 3.3	7.7 ± 2.3	8.4 ± 2.5	8.4 ± 2.4
	2	9.7 ± 1.9	9.3 ± 2.2	11.4 ± 2.8	10.0 ± 3.5	9.2 ± 2.6	9.9 ± 2.7	10.0 ± 2.4
	3	12.1 ± 3.6	11.8 ± 3.2	13.3 ± 4.7	10.6 ± 3.8	10.8 ± 3.4	11.7 ± 3.8	11.9 ± 3.6
	4	13.5 ± 4.3	11.8 ± 3.9	14.9 ± 3.8	11.5 ± 3.9	11.4 ± 3.6	12.6 ± 4.0	12.6 ± 3.6
	All	10.9 ± 3.5	10.3 ± 3.2	12.3 ± 3.9	10.3 ± 3.6	9.8 ± 3.2	10.7 ± 3.6	10.8 ± 3.3

Blood parameters reveal no marked dependence on BIRADS category or measurement position. The total hemoglobin content *tHb* increases slightly with mammographic density (as shown in Table 6). Blood oxygenation SO_2 shows neither progressive change with BIRADS category nor systematic dependence or position, with average value of 87%. Thus, blood volume and oxygenation are not further considered for the estimate of breast density.

Some differences in the average values of optically derived parameters are observed also between left and right breasts. As recently reported in the literature, asymmetry in breast density might be a strong indicator of cancer risk [12]. Thus, the apparent difference between

#174025 - $15.00 USD Received 8 Aug 2012; revised 3 Sep 2012; accepted 3 Sep 2012; published 6 Sep 2012

left and right breast was further analyzed evaluating the potential correlation between optically derived parameters estimated at any of the five locations on one breast and the corresponding value on the controlateral breast. Since breast density is the risk factor under investigation, we considered all parameters that correlate significantly with breast density in our studies (Ref. [6] and further unpublished data): water, collagen, lipid and scattering power. Comparable values between left and right breasts (paired t-test, $p > 0.05$) were obtained for water, collagen and lipid content. On the contrary, a statistically significant difference (paired t-test, $p < 0.01$) was observed for the scattering power b, which seems to be consistently higher in the right breast at any measurement positions. The situation seems not to change appreciably if 13 patients with lesions are excluded from the population. However, for its potential interest as a risk factor, bilateral asymmetry in optically derived parameters will be further investigated separately, when data on a higher number of subjects is available.

As shown in Tables 2–5, for any of the four parameters the average over each of the five areas gives results that are comparable with what obtained performing an average over full scan data. This suggests that the 5 areas considered here are able to fully sample the heterogeneous breast tissue, at least for what concerns average properties.

The effectiveness of measurements performed on a small area for the assessment of mammographic density was tested using the synthetic Optical Index *OI*, which combines as follows all parameters that showed significant dependence on breast density [8]:

$$OI = \frac{[\text{water}][\text{collagen}]b}{[\text{lipid}]}. \quad (1)$$

Table 7 reports the *OI* values as a function of measurement position and BIRADS category. On average, a progressive and marked increase is observed with breast density.

Table 7. Optical Index *OI* as a function of measurement position and BIRADS category[a]

BIRADS category	1 Outer	2 Chest	3 Inner	4 Nipple	5 Middle	All areas	Full scan
1	1.9 ± 0.5	1.4 ± 0.6	1.4 ± 0.4	2.2 ± 1.1	1.5 ± 0.6	1.6 ± 0.6	1.9 ± 1.0
2	4.1 ± 3.0	4.3 ± 7.7	3.0 ± 3.4	4.0 ± 2.1	2.8 ± 1.6	3.5 ± 3.8	4.8 ± 5.0
3	29 ± 34	17 ± 16	10 ± 10	31 ± 34	20 ± 21	21 ± 25	26 ± 27
4	166 ± 81	149 ± 63	79 ± 45	211 ± 90	164 ± 65	152 ± 76	146 ± 84

[a]The data are averaged over the left and right CC views.

Table 8. Effectiveness of the Optical Index *OI* in discriminating different BIRADS categories. p values of the Mann-Whitney test are used as a measure the effectiveness[a]

BIRADS category	1 Outer	2 Chest	3 Inner	4 Nipple	5 Middle	All areas	Full scan
2 *vs* 1	0.0078	*0.0705*	*0.1162*	0.0058	0.0040	0.0016	0.0058
3 *vs* 2	0.0018	0.0001	0.0005	0[b]	0.0001	0	0
4 *vs* 3	0.0006	0.0003	0.0002	0.0002	0.0002	0.0002	0.0001

[a]Cases where statistical significance is not achieved are reported in Italic.
[b]Output as provided by the statistical software Minitab 15 when $p < 0.0001$

For measurements performed in areas 2 (Chest) and 3 (Inner), the spreading of *OI* values classified in BIRADS category 2 likely causes partial overlap with BIRADS category 1. Thus, as shown in Table 8, subjects belonging to the two lowest density categories cannot be effectively discriminated. However, even data collected from areas 2 (Chest) and 3 (Inner) can identify high risk subjects (category 4 and possibly 3). Apart from this, *OI* values estimated from measurements carried out at any position on subjects belonging to distinct BIRADS categories are always statistically different with high significance, indicating that a single point optical measurement can provide an effective noninvasive assessment of breast density. This outcome can likely be attributed to the strongly diffusive nature of breast tissue that

#174025 - $15.00 USD Received 8 Aug 2012; revised 3 Sep 2012; accepted 3 Sep 2012; published 6 Sep 2012

makes it possible to probe several cm^3 of tissue even injecting and collecting light from a small area.

It should be taken into account that data were acquired with acquisition time of 25 ms/mm^2). Thus, the overall measurement time for the 5 mm × 5 mm area considered here is less than 1 s (*i.e.*, 625 ms), corresponding at most to 1.25×10^5 counts/wavelength.

In particular, the middle area seems to be specially promising for the classification of breast density. In fact, the measurement should be performed in the middle of the breast volume, in a position that is far from boundaries, which might cause artifacts if they are too close. Moreover, other neighbor areas (*i.e.*, areas 1 and 4) still provide acceptable results, relaxing the constraints on the exact location of the measurement probe.

It is also interesting to note that a single measurement performed in area 5 (Middle) is only slightly less effective than full scan measurements and that the average over the 5 areas provides results that are comparable to what obtained from full scan data. Only one exception appears: the average over the 5 areas seems to be more effective than the full scan in the discrimination between category 1 and 2. This might be due to the fact that, even though regions that are too close to the breast boundary are excluded from the analysis of full scan data, some points that are partly affected by "boundary effects" might still be included and limit the possibility to discriminate between BIRADS categories. This effect becomes significant only between category 1 and 2 that are more difficult to separate by optical means.

4. Conclusions

We have shown previously that optically derived parameters obtained from full scan breast data can estimate breast density in good agreement with BIRADS categories. A synthetic optical index was also introduced to improve the assessment of breast density by combining all parameters that correlate significantly with it.

The present work shows that full scans are not needed and single point measurements perform comparably in the assessment of breast density. This was proved by averaging data collected over small areas (5 mm × 5 mm), which is essentially equivalent to performing a single measurement with a 5 mm fiber bundle. Moreover, the choice of the probe position on the breast seems not to be critical. Our findings are in agreements with the results obtained by Lilge's group: even though with a different experimental approach, they applied effectively transmittance measurements carried at single acquisition points for the optical assessment of mammographic density [5,6].

These outcomes are promising for routine clinical application of the optical estimate of breast density, as they significantly downscale the requirements on both needed instrumentation and measurement procedure. Actually, no breast scanning is required, which reduces significantly technical complexity, costs and measurement times. Moreover, the measurement should be performed in the middle of the breast volume, far from boundaries that might affect negatively data analysis, and the exact measurement location is not critical, as already mentioned.

Finally, it is worth noting that, due to limitations in the maximum acceptable time for the measurement of entire breast images, data examined in the present study were collected with very short acquisition time. If just a single measurement is performed, longer acquisition times become accessible. The consequently higher signal level might further improve the quality of the data and the correlation between optically derived parameters and mammographic density.

Overall, these findings pave the way to the development of compact devices for an easy and fast noninvasive assessment of breast density. Due to the limited cost, such devices might have widespread application, with high impact on public health (including personalized diagnostic paths and prevention interventions for high-risk women).

#174025 - $15.00 USD Received 8 Aug 2012; revised 3 Sep 2012; accepted 3 Sep 2012; published 6 Sep 2012

Acknowledgments

The authors wish to acknowledge partial support from the European Community's Seventh Framework Programme (FP7/2007-2013) under grant agreement 284464 (LASERLAB-EUROPE).

#174025 - $15.00 USD Received 8 Aug 2012; revised 3 Sep 2012; accepted 3 Sep 2012; published 6 Sep 2012